Timed Verification of the Generic Architecture of a Memory Circuit Using Parametric Timed Automata ⋆ ⋆⋆

Remy Chevallier[1], Emmanuelle Encrenaz-Tiphene[2], Laurent Fribourg[2] and Weiwen Xu[2]

[1] STMicroelectronics, FTM, Central R&D, Crolles, France
[2] LSV - CNRS, ENS de Cachan, France

Abstract. Using a variant of Clariso-Cortadella's parametric method for verifying asynchronous circuits, we analyse some crucial timing behaviors of the architecture of SPSMALL memory, a commercial product of STMicroelectronics. Using the model of parametric timed automata and model checker HYTECH, we formally derive a set of linear constraints that ensure the correctness of the response times of the memory. We are also able to infer the constraints characterizing the optimal setup timings of input signals. We have checked, for two different implementations of this architecture, that the values given by our model match remarkably with the values obtained by the designer through electrical simulation.

Keywords. Memory Circuit, Timed Automata, Model Checking.

⋆ Partially supported by project MEDEA+ Blueberries.

⋆⋆ A preliminary version appeared in the Proceedings of 4th International Conference on Formal Modelling and Analysis of Timed Systems (FORMATS'06), Sept. 2006.

1 Introduction

The designer of a memory circuit guarantees the correct behavior of its product and some quantitative performance (called "(guaranteed) response times"), assuming that the circuit is embedded into an environment satisfying some quantitative requirements (called "(external) requirements"). The response times represent an upper bound on the time taken by the circuit to produce the result of a (write or read) operation. The external requirements specify the lower bounds on the clock cycle times and the stability times of input signals. These values of the parameters of the specification form the *datasheet* of the circuit provided by the manufacturer to the customer. They are determined by *electrical simulation*. In order to perform such a simulation, each component of the memory is modelled at the transistor level as a set of differential equations, which represent the Kirchoff laws associated with the electric current traversing the component. These differential equations depend on the physical characteristics of the transistors and wires (capacitors, resistors, ...). The full memory is thus represented as a big system of differential equations. The values of the datasheet are computed by resolution of these differential equations, using, e.g., tool HSIM [1]. Actually, such a simulation process is much too long to be performed in a complete manner. Sensitive portions of the circuit, which are supposed to contain the longest paths of traversal, are therefore identified by hand. Electrical simulations are performed only for such limited portions of circuit, which are assumed to contain the critical paths. Such an assumption of 'criticality' is risky: it is very difficult to identify by hand relevant sensitive portions of the circuit (especially when the complexity of the circuit increases). The need for *formal methods* to verify the timing values of the datasheet is therefore widely recognized.

In [9, 8], Clariso and Cortadella propose a formal method for verifying the timings of asynchronous circuits. The approach infers a set of sufficient linear constraints relating the delays of the internal gates of the circuit to the external delays of the circuit specification that guarantee the correct behavior of the circuit. The method is based on the reachability analysis of a timed model of the circuit (with additional abstract interpretation techniques [10]). As pointed out in [9], such parametric constraint sets are very informative for the designer, as they identify sensitive parts of the circuits (e.g., "critical paths") and interrelations between various data of the specification. Moreover, many technology mappings can be tested immediately (by mere instantiation of the parameters). We follow here a similar approach for formally verifying some generic properties of a commercial memory designed by STMicroelectronics, called SPSMALL. Our timing analysis method derives a set of sufficient linear constraints relating the external parameters of the datasheet to the internal gate delays that guarantee the correctness of the circuit's behavior. In particular, these constraints can be seen as sufficient conditions for certain paths of the circuit to be "critical" (i.e. those along which the propagation delay is the longest). Using the model of parametric timed automata (see [3]) and tool HYTECH [13] for reachability analysis, we are able to generate a set of linear constraints that ensures the correctness

of some crucial timing behaviors of the memory. This method is applicable to several instances of SPSMALL memories implemented with different transistor technologies (corresponding to different sets of parameter values). We actually applied the method to two instances, called $SP1$ and $SP2$, which correspond to a high-speed and low-power implementations respectively.

Comparison with Related Work. As pointed out above, our work is adapted from Clariso-Cortadella's method [9, 8]. However, [9, 8] focus on a particular form of linear constraints (linear inequalities with coefficients always equal to ± 1) and represent them as a particular form of convex polyhedra, called "octahedra" [8]. In contrast, we use here linear constraints and their classical form of convex polyhedra in their full generality [12]. Other differences with [9, 8] are:

- a different level of modelling: the components of the memory are represented here at the "latch" level instead of gate level. At this level of representation, the flow of input signals traverses the circuit in a linear manner (without loops), while the flow is cyclic at the gate level (the ouput of one gate can be an input of another gate and the converse can be simultaneously true),
- the use of mere forward reachability analysis rather than techniques of fixpoint computation of abstract interpretation (using, e.g., widening operators),
- the use of a decompositional approach, which splits the global system into three smaller parts,
- the use of a *step-by-step refinement* of the reachability analysis process: we start with the most general form of constraints on parameters; we then refine them progressively, via *iterative* reachability analysis, detecting, at each run, some erroneous generated states until complete elimination.

Besides [9, 8], our work is along the lines of [15, 5, 17] where timed automata have been used extensively to model and check timing properties of asynchronous circuits (cf. [11]). Reachability analysis is there performed via tool KRONOS [18]. Our work is also a continuation of [4, 7] where the SPSMALL memory is modelled as a timed automaton and some of its timing properties are proven by reachability analysis (using tool UPPAAL [14]). The crucial difference here, with respect to these previous works, is that we use the model of *parametric* timed automata (performing reachability analysis with HYTECH [13]).

Plan of the paper. In Sect. 2, we present the general objectives of our verification process. We explain in Sect. 3 how a high-level description of the memory circuit is transformed in a timed automaton. We then give a general description of our method of analysis (Sect. 4). In Sect. 5, the method is applied to verify the write property of the SPSMALL memory after a preliminary split of the model into 3 parts. The counterpart results for the read property are given in Sect. 6. Final remarks are given in Sect. 7.

2 Statement of the Problem

2.1 Architecture of a Memory Circuit

A memory circuit aims at storing data at some addressed locations. It is associated with two operations: 'write' and 'read'. The memory circuit has several input ports and one output port (see Fig. 1). The signals driven by input ports are:

- CK, the signal of the periodic clock;
- D, the n-bits width signal representing the data to be stored;
- A, the $\log_2(m)$-bits width signal representing the address of an internal memory location;
- WEN, the 1-bit width signal representing either a write or a read operation.

The signal driven by the output port is Q (of n-bits width). The data are stored in a memory array composed of $m \times n$ memory points. A memory location is a collection of n memory points. This is depicted on Fig. 1. The write operation ($WEN = 0$ when CK is rising) writes the value of D in the internal memory location selected by A, and propagates D on output port Q. The read operation ($WEN = 1$ when CK is rising) outputs on port Q a copy of the data stored in the memory location selected by A.

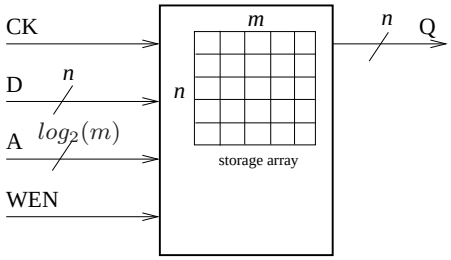

Fig. 1. Simplified view of a memory (Symbol $-\!\!\not{|}^{k}\!\!\rightarrow$ represents a port of k-bits width)

2.2 Simplification

As a simplification, we will consider the case where the ports of D are reduced to a single bit. The propagation of all the bits of D follow identical paths. Each path propagates either a rising edge or a falling edge. Let us point out that the propagation time of a rising edge *differs* from that of a falling edge. However, the propagation of all the rising (resp. falling) edges takes the same time. This justifies the reduction of our model to a datapath of one bit for D, with *two* cases depending on whether D is rising or falling. Accordingly, the same simplification

is done for Q.

A similar reduction applies to A: first, all the bits of A follow identical paths before reaching the address decoder; then, all the paths in the address decoder are abstracted as the "slowest" path (the one taking the longest time to propagate the signal).

Likewise, we are naturally led to focus to a unique memory point, denoted by mp, instead of the original $m \times n$ storage array. Note that the operations involving the original $m \times n$ memory points may take different times, depending on their physical location. Our abstraction is justified because we will assume that mp corresponds to the point of the storage array from which the *slowest* path to Q originates (See Sect. 6).

A closer view of the storage mechanism is given in Appendix 1.It highlights the reduction of parallel paths for D, A and Q. For more details about memory architecture, see [16].

2.3 Timings

A memory is embedded into a synchronous environment scheduled by a periodic signal, named 'clock' (CK). The period of a cycle, t_{cycle}, decomposes itself into a high period (t_{HI}) and a low period (t_{LO}). In order to be taken into account, each input signal I has to remain stable for a given amount of time, before the rising edge of the clock. This delay is called *setup* time for I, and denoted by t_{setup_I}[3].

Traversal of internal components. The circuit is made of a number elementary internal components (logical gates, latches, wires,...). The logical gates (or blocks) are assumed to be traversed instantaneously[4]. The only components with non-null delay are the wires and the latches. Each wire and latch component is associated with an interval $[l^{\uparrow}, u^{\uparrow}]$ (resp. $[l^{\downarrow}, u^{\downarrow}]$), which gives lower and upper bounds of the component traversal delay when the attacking signal is rising (resp. falling)[5]. We adopt the "*inertial* delay" interpretation (see [6]): changes that do not persist for l time are filtered out.

Actual response times. A write operation occurs when input signal WEN is low. Due to the time of traversal of the elementary components of the memory, this operation takes a delay, called "actual response time for write", denoted by $t_{CK \to Q}^{D,WEN\downarrow}$. This is depicted on Fig. 2. Due to the one-bit abstraction of D,

[3] There exists also a required delay of stability, called "hold" time, required *after* the rising edge of the signal, but we will not consider it in this paper.

[4] If the delay of traversal of the gate is non-null, we backpropagate it to the input wires of the gate (cf. [15]).

[5] This is a straightforward generalization of "*bi-bounded* delay" model (see [6]), taking into account the rising or falling nature of input signal.

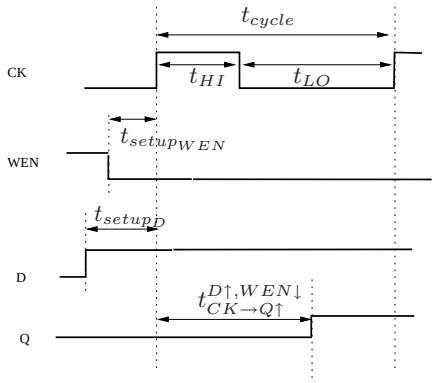

Fig. 2. A *write* operation corresponding to a rising edge of D ($D\uparrow$).

this delay now just depends on whether D is rising or falling. A rising (resp. falling) edge of D induces a rising (resp. falling) edge of Q. Accordingly, this delay will be denoted by $t^{D\uparrow,WEN\downarrow}_{CK\to Q\uparrow}$ or $t^{D\downarrow,WEN\downarrow}_{CK\to Q\downarrow}$. The delay $t^{D,WEN\downarrow}_{CK\to Q}$ is just the maximum of these two values.

Similarly, when a read operation occurs ($WEN = 1$), the "actual response time for read", denoted by $t^{A,WEN\uparrow}_{CK\to Q}$, can be defined along the same lines. This delay is itself the maximum of the values corresponding to the falling and rising edges of A, denoted by $t^{A\uparrow,WEN\uparrow}_{CK\to Q\uparrow}$ and $t^{A\downarrow,WEN\uparrow}_{CK\to Q\downarrow}$ respectively.

Response times guaranteed by the datasheet. The datasheet states the maximum delay, denoted by t^{write}_{max}, after which a write operation is guaranteed to have produced its result. A similar delay, denoted by t^{read}_{max}, is also given for the read operation. The values t^{write}_{max}, t^{read}_{max} form the *(guaranteed) response times* part of the datasheet.

The setup and cycle timing values ($t_{HI}, t_{LO}, t_{setup_D}, t_{setup_A}, t_{setup_{WEN}}$) form the *(external) requirements* of the datasheet.

2.4 Verified properties

We suppose that we are given an implementation of the memory, and assume that its environment satisfies the external requirements of the datasheet. We are interested in verifying that the actual response times are no greater than the corresponding response times guaranteed by the datasheet.

Write property. The result of a *write* command is produced on output port Q within t^{write}_{max}. This will be expressed as: $t^{D,WEN\downarrow}_{CK\to Q} \leq t^{write}_{max}$.

Read property. Similarly, we will express the correctness of a read command as: $t_{CK \to Q}^{A,WEN\uparrow} \leq t_{max}^{read}$.

Optimal setup timings. Besides, our analysis will allow us to infer an optimal value for setup timing t_{setup_D} (resp. t_{setup_A}): it corresponds to the lowest value of t_{setup_D} (resp. t_{setup_A}) which still guarantees the read and write properties, while letting invariant the values of all the other parameters of the datasheet.

3 Modelling

We suppose that we are given a high-level description of the memory circuit under the form of an abstract (timed) functional graph (see Fig. 3). Given such a graph, we explain how to transform it into a timed automaton.

3.1 Level of Modelling.

A memory can be modelled at different levels of complexity, e.g., in an increasing order: at the functional block level, at the "latch" level, at the gate level, or at the transistor level. For the SPSMALL memory, the model can thus be implemented using: 3 main components, at the block level (cf [4]), 30 components at the latch level, 70 components at the gate level, or 200 components at the transistor level. There is a tradeoff in finding the appropriate level of modelling. The lower the level of modelling is, the more faithful to the reality the model is, but the more difficult the verification process is.

In this work, we chose to represent the memory at the latch level. The advantage is to limit the number of components (around 30) at a reasonable size, and to have a "schematics" describing the architecture of the memory at this level, which closely corresponds to (VHDL) code automatically produced with the commercial tool TLL [2]. This is depicted on Fig. 3. The schematics naturally decomposes into two relevant subparts, depending on whether one studies the circuit on a write or read operation. These parts are depicted on Fig. 7 and Fig. 8 for write and read respectively. Each part is made of three kinds of components: wires, latches and logical blocks:

- A *wire* carries an input signal to its output with a delay in $[l^{\uparrow}, u^{\uparrow}]$ (resp. $[l^{\downarrow}, u^{\downarrow}]$).
- A *latch* is a component that can store one bit of data. It has two inputs d (*data to be latched*) and e (*enable*), and one ouput q. It propagates the input data d to its output q (with a delay in $[l^{\uparrow}, u^{\uparrow}]$ or $[l^{\downarrow}, u^{\downarrow}]$) as long as e is high. While e is low, q keeps its value (even if d changes). The latch is said to be "closed" (resp. "open") when $e = 0$ (resp. $e = 1$).
- Logical blocks are used to output a signal fonctionally dependent of the inputs of the block. (Recall that we assume in this paper that the delays associated with such blocks are null.)

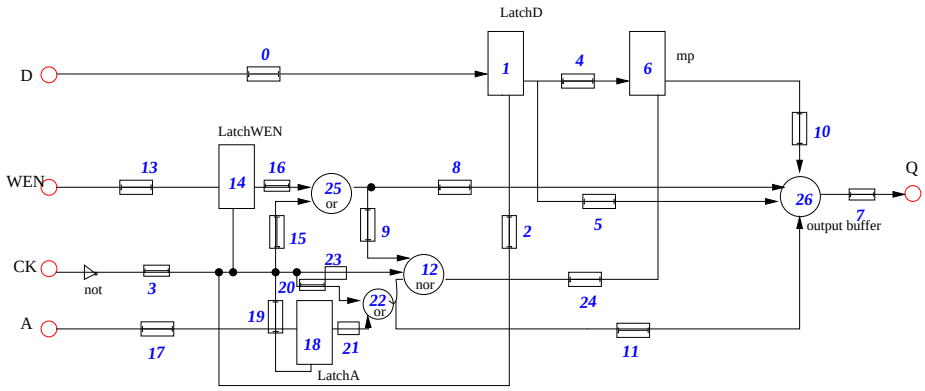

Fig. 3. Abstract graph for SPSMALL

3.2 SPSMALL as a Timed Automaton.

The model of timed automata [3] is especially well-suited to represent asynchronous circuits (see, e.g., [15, 5, 17]). Roughly speaking, a timed automaton is a finite state automaton enriched with *(symbolic) clocks* that evolve at the same uniform rate, and can be reset to zero. A *state* is a pair (ℓ, v) where ℓ is a *location* (or "control state"), and v a clock valuation. Each location is associated with a conjunction of linear constraints over clocks, called *invariant*. A state (ℓ, v) has a *discrete transition*, labelled e, to (ℓ', v') if v satisfies a constraint, called *guard*, associated to e, and v' is obtained from v by resetting some clocks to 0. The state (ℓ, v) has a *time transition* of duration t to (ℓ, v') if $v' = v + t$ and for all t' $(0 \leq t' \leq t)$, $v + t'$ satisfies the invariant associated to ℓ. States can be expressed under the symbolic form of conjunctions of linear constraints. Such states are classically represented as convex polyhedra (see, e.g., [13]). Sets of states correspond to unions of polyhedra. The *(forward) reachability analysis* consists in generating iteratively the "successors" of sets of states via the system transitions, using elementary manipulation of polyhedra.

The SPSMALL memory is modelled as a timed automaton, resulting from the composition of all the timed automata corresponding to the input signals and the internal components. More precisely:

- Each input signal of the memory (synchronous signal CK, input signal D, read/write command WEN) is represented as a timed automaton.
- Each component of the memory (latch, wire, ...) is also represented as a timed automaton,
- The transmission of an internal signal between two components is modelled by synchronizing the two corresponding timed automata via a shared discrete transition.

Let us explain how to model a wire as a timed automaton. The wire component is enabled $l^{\uparrow}$ (pico)secs after the rising edge of the input signal, and the output signal is fired after a delay lying in $[l^{\uparrow}, u^{\uparrow}]$ (parameters $l^{\uparrow}$ and $u^{\uparrow}$ are used to propagate a falling edge). Such a wire component is naturally modelled as the timed automaton depicted in Fig. 4. It makes use of 1 internal clock c and 5 locations. The symbol $d\uparrow$ (resp. $d\downarrow$) corresponds to a rising edge (resp. falling edge) of input internal signal d, and similarly for symbol $o\uparrow$ (resp. $o\downarrow$) with output signal o. Each edge corresponds to a discrete transition labelled with the name of input signals ($d\uparrow$ or $d\downarrow$) or output signals ($o\uparrow$ or $o\downarrow$). The medium-level locations are associated with invariants $c \leq u^{\uparrow}$ or $c \leq u^{\downarrow}$. The guard associated with edges outgoing downwards from these locations is $c \geq l^{\uparrow}$ or $c \geq l^{\downarrow}$.

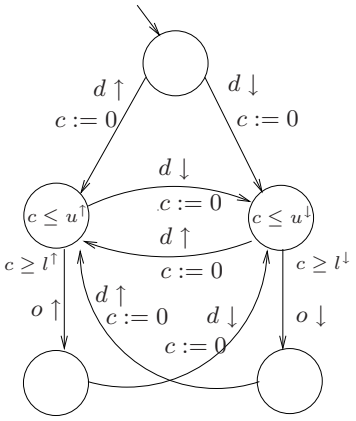

Fig. 4. Timed automaton of a wire component with delays $[l^{\uparrow}, u^{\uparrow}]$ and $[l^{\downarrow}, u^{\downarrow}]$ to propagate an edge from d to o.

Likewise, a latch is modelled as a timed automaton depicted on Fig. 5 (using the same conventions as for the wire automaton). There are 6 locations and 1 clock c. The name of the locations $e_i d_j$ reflects the values i and j of e and d respectively; besides $e_1 d_j B$ indicates that an output $q\uparrow$ (resp. $q\downarrow$) has already been produced if $j = 1$ (resp. $j = 0$).

4 Analysis

We now analyse the timed automaton modelling the memory. Roughly speaking, the analysis process then consists to:

– generate the set of reachable states (within a finite number of cycles, *viz.* 2 cycles),

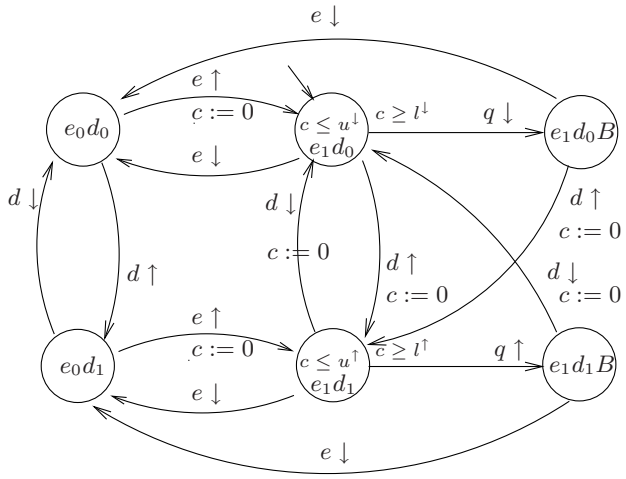

Fig. 5. Timed automaton of a latch component with delays $[l^{\uparrow}, u^{\uparrow}]$ and $[l^{\downarrow}, u^{\downarrow}]$ to propagate an edge from d to q.

- infer (by stepwise refinement) a set of timing constraints ensuring the response time property,
- verify that, for a given implementation, the response time property holds by checking the instantiated constraints.

In Sect. 4.1, we first explain the process at the *instance* level: all the parameters are supposed to be instantiated with constants. In Sect. 4.2, we explain how the whole process is performed at the *generic* level (no parameter is instantiated).

4.1 Reachability Analysis at the Instance Level

We consider here that we are given a specific implementation of the SPSMALL memory, e.g. $SP1$. We suppose that all the parameters are instantiated either with the values of the datasheet $SP1$ (for t_{HI}, t_{LO}, t_{setup_D}, $t_{setup_{WEN}}$, t^{write}_{max}, t^{read}_{max}) or with the values found by simulation (for the internal component delays $\{[l_i^{\uparrow}, u_i^{\uparrow}]\}$ and $\{[l_i^{\downarrow}, u_i^{\downarrow}]\}$). All the parameters are thus considered here as constants.

A "global clock" s (which is initialized to 0, and never reset) is used to measure the evolution of time. In order to verify property: $t^{D\uparrow,WEN\downarrow}_{CK\rightarrow Q\uparrow} \le t^{write}_{max}$, we model the behavior of the memory along two cycles:

- a 1st cycle where the values of D and WEN are set t_{setup_D} and $t_{setup_{WEN}}$ time before the 2nd rising edge of CK (corresponding to the write operation); input signal WEN is modelled as a falling edge, followed by a low level (selection of a write command), and input signal D is modelled as a rising

edge, followed by a high level (in keeping with the stabilization requirement $setup_D$).
– a 2nd cycle where the write operation is performed (the D value is propagated on Q port).

Accordingly, the observation of the generated states is done along two cycles (see Fig. 6).

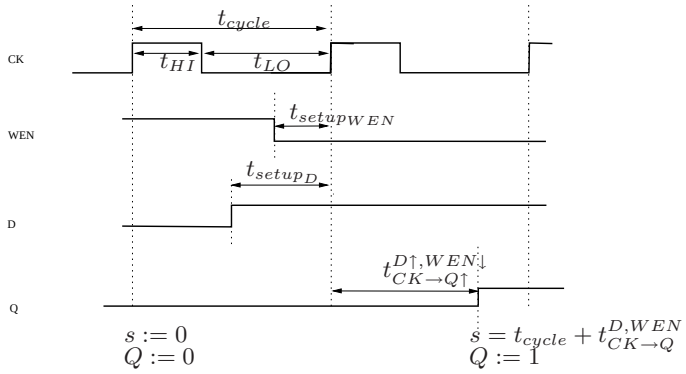

Fig. 6. The *write* operation used in our experiment.

We use a flag (initialized to 0) which stores the fact that the rising edge of input signal D has reached Q port. This flag will also be denoted by Q. The value of s when Q is set to 1, corresponds to the sought value $t^{D\uparrow,WEN\downarrow}_{CK\rightarrow Q\uparrow}$. Starting from $s = 0 \wedge Q = 0$, the set of reachable states is iteratively computed until, either:

– the switch of Q occurs before 2 cycles, or
– 2 cycles are run out without any switch of Q.

This yields a set of final states, denoted by $Post^{2t_{cycle}}$, which can be decomposed into:

– *good* states, i.e, states, for which the switch of Q has occurred ($Q = 1 \wedge s = t_{cycle} + t^{D\uparrow,WEN\downarrow}_{CK\rightarrow Q\uparrow} \leq 2t_{cycle}$).
– *bad* states, i.e., states, for which 2 cycles has run out without any switch of Q ($Q = 0 \wedge s = 2t_{cycle}$).

The property holds iff:

– all the final states of $Post^{2t_{cycle}}$ are good (no bad state), and
– for each final state, the value $t^{D\uparrow,WEN\downarrow}_{CK\rightarrow Q\uparrow}$ of s is at most equal to t^{write}_{max} (i.e.: $t^{D\uparrow,WEN\downarrow}_{CK\rightarrow Q\uparrow} \leq t^{write}_{max}$).

The symmetrical property: $t^{D\downarrow,WEN\downarrow}_{CK\rightarrow Q\downarrow} \leq t^{write}_{max}$ has to be also verified. This is done along the same principles as described above.

4.2 Reachability Analysis at the Generic Level

In contrast with Sect. 4.1, the timings of the datasheet (*viz.*, t_{HI}, t_{LO}, t_{setup_D}, $t_{setup_{WEN}}$, t^{write}_{max}, t^{read}_{max}) as well as the internal component delays $\{[l_i^{\uparrow}, u_i^{\uparrow}]\}$, $\{[l_i^{\downarrow}, u_i^{\downarrow}]\}$ are now kept uninstantiated, and can be seen as *timing parameters*. Each state generated by reachability analysis corresponds to a conjunction of inequalities of the form $\rho \leq \sigma$ or $\rho < \sigma$, where ρ and σ are linear terms involving the clock variable s, the variable $t^{D\uparrow,WEN\downarrow}_{CK\rightarrow Q\uparrow}$ and the timing parameters.

We suppose given an implementation of the SPSMALL memory, say $SP1$, and will derive a set of constraints, say $Assumption(D\uparrow)$, over the parameters that *generalizes* the values of $SP1$. (In other words, the values of $SP1$ will satisfy $Assumption(D\uparrow)$.) At the beginning of the process, $Assumption(D\uparrow)$ is $True$, which means that we start with the most general parameters ($l_i^{\uparrow}$ (resp. $l_i^{\downarrow}$) is just assumed to be less than or equal to $u_i^{\uparrow}$ (resp. $u_i^{\downarrow}$)). Given an initial set of states characterized by $Assumption(D\uparrow)$, we perform reachability analysis on 2 cycles. We thus generate a set of constraints, denoted by $Post^{2t_{cycle}}(Assumption(D\uparrow))$. The first run of $Post^{2t_{cycle}}(Assumption(D\uparrow))$, with $Assumption(D\uparrow) = True$, usually contains bad (final) states. The *refinement* process consists in eliminating such bad states, by restricting the possible values of the parameters, as follows:

1. select a bad state, say B, of $Post^{2t_{cycle}}(Assumption(D\uparrow))$;
2. identify a "transgressing inequality", say J, of B, i.e., a conjunct of B that is violated by the values of an SPSMALL available instance (*viz*, $SP1$).[6]
3. add the negation of J to $Assumption(D\uparrow)$.
4. Recompute $Post^{2t_{cycle}}(Assumption(D\uparrow))$ after having reset s and Q to 0.

And so on, perform iteratively 1-2-3-4 until no bad state is generated.

At each run, $Assumption(D\uparrow)$ is a conjunction of linear inequalities with an increasing number of conjuncts. Accordingly, $Post^{2t_{cycle}}(Assumption(D\uparrow))$ decreases at each run. At the end, the refinement process outcomes two formulas, $Assumption(D\uparrow)$ and $Final(D\uparrow) \equiv Post^{2t_{cycle}}(Assumption(D\uparrow))$:

- $Assumption(D\uparrow)$ is a conjunctive constraint binding parameters of the external requirements of the datasheet (cycle and setup timings) to the internal component delays $\{[l_i^{\uparrow}, u_i^{\uparrow}]\}, \{[l_i^{\downarrow}, u_i^{\downarrow}]\}$.
- $Final(D\uparrow)$ is a set of conjunctive constraints relating the actual response time $t^{D\uparrow,WEN\downarrow}_{CK\rightarrow Q\uparrow}$ to the internal component delays $\{[l_i^{\uparrow}, u_i^{\uparrow}]\}, \{[l_i^{\downarrow}, u_i^{\downarrow}]\}$.

Typically, $Final(D\uparrow)$ is of the form:

$f(\overline{l}, \overline{u}) \leq t^{D\uparrow,WEN\downarrow}_{CK\rightarrow Q\uparrow} \leq g(\overline{l}, \overline{u})$,

where $f(\overline{l}, \overline{u})$ and $g(\overline{l}, \overline{u})$ are linear expressions over the delays $l_i^{\downarrow}, u_i^{\downarrow}, l_i^{\uparrow}, u_i^{\uparrow}$ associated to all the components i of the system.

[6] An example of transgressing inequality is given in Appendix 2.

By construction, *Final*($D\uparrow$) contains good states only (the writing always occurs within two cycles). Given an implementation of the memory, *Assumption*($D\uparrow$) and *Final*($D\uparrow$) can now be used to show that $t_{CK\rightarrow Q\uparrow}^{D\uparrow,WEN\downarrow} \leq t_{max}^{write}$ is satisfied. This is done by checking that, after instantiation of all the parameters with the values of the datasheet and the values of the internal delays of the implementation:

1. *Assumption*($D\uparrow$) holds;
2. $Final(D\uparrow)$ entails $t_{CK\rightarrow Q\uparrow}^{D\uparrow,WEN\downarrow} \leq t_{max}^{write}$.

Note that, in the case where $Final(D\uparrow)$ is of the form $f(\overline{l},\overline{u}) \leq t_{CK\rightarrow Q\uparrow}^{D\uparrow,WEN\downarrow} \leq g(\overline{l},\overline{u})$, checking item 2 reduces to check: $g(\overline{l},\overline{u}) \leq t_{max}^{write}$.

In an analogous way, in order to verify the counterpart property for the falling edge of D, one will infer *Assumption*($D\downarrow$) and *Final*($D\downarrow$), and will check: $t_{CK\rightarrow Q\downarrow}^{D\downarrow,WEN\downarrow} \leq t_{max}^{write}$. From $t_{CK\rightarrow Q\uparrow}^{D\uparrow,WEN\uparrow} \leq t_{max}^{write}$ and $t_{CK\rightarrow Q\downarrow}^{D\downarrow,WEN\downarrow} \leq t_{max}^{write}$, one infers that the implementation satisfies:
$t_{CK\rightarrow Q}^{D,WEN\downarrow} \leq t_{max}^{write}$.

Sets *Assumption*($D\uparrow$) and *Assumption*($D\downarrow$) can also be used to find the constraints associated to the *optimal* setup timing t_{setup_D}: it corresponds to the lowest value of t_{setup_D} which still guarantees the read and write properties, while letting invariant the values of all the other parameters of the datasheet. This is illustrated in Sect. 5.2.

5 Verification of the Write Property of SPSMALL

We apply the method for proving the correctness of the timings of the datasheet of SPSMALL for the write operation. The relevant portion of this schematics for the write property is described on Fig. 7. Note that, somehow surprisingly, the memory point *mp* is absent of the schematics: the write property concerns an end-to-end propagation of information from D to Q, which actually *bypasses* the memory point (where D is independently stored)[7]. The schematics contains 14 components: 8 "wire" components, which transmit an input; one "not" component, which transmits the negation of its input ; one "or" component which computes the logical "or" of its two inputs, one functional block representing the output buffer and two "latches", $latch_D$ and $latch_{WEN}$.

We now apply the above method for deriving the sets *Assumption*($D\uparrow$) and *Final*($D\uparrow$) of constraints associated with memory SPSMALL, in the case of a rising edge of D. A similar approach applies for the case of a falling edge.

5.1 Decomposition

The relevant portion of the circuit for the write command from D to Q has been depicted on Fig. 7. In practice, we cannot apply directly the method described

[7] Such a bypass mechanism is a feature of so-called "write-through" memories.

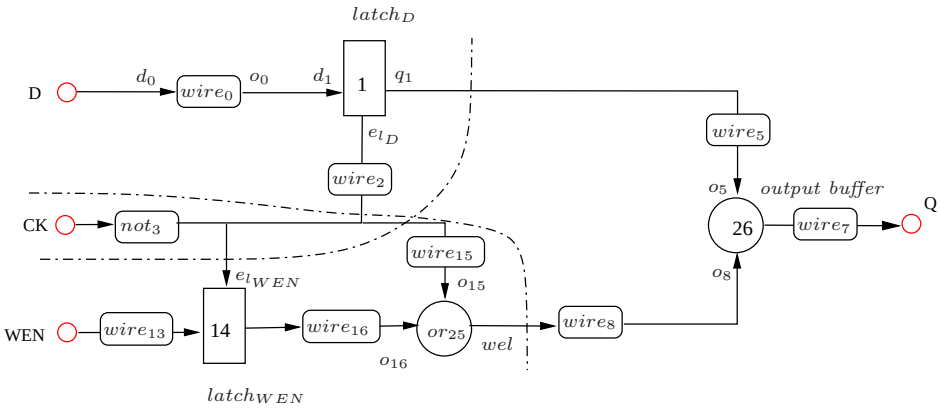

Fig. 7. Schematics of the relevant portion of SPSMALL for write.

above, because we cannot perform reachability analysis with HYTECH due to the high number (34) of parameters. The model is therefore decomposed into three parts (see the dashed lines on Fig. 7):

- The 1st part represents the D's edge propagation through $latch_D$: The input signals are D and CK. The output is the output of $latch_D$, denoted by q_1. A rising edge of D induces a rising edge on q_1. The goal is to compute lower and upper bounds of the occurrence time of the rising edge of q_1, starting from the rising edge of CK. This delay will be denoted by $t^{D\uparrow}_{CK\rightarrow q_1\uparrow}$.
- The 2nd part represents the propagation of the WEN falling edge through $latch_{WEN}$ (among other components). The input signals are WEN and CK. The output is denoted by wel. A falling edge of WEN induces a falling edge on wel. The goal is to compute the lower and upper bounds of the occurrence time of the falling edge of wel, starting from the rising edge of CK. This delay will be denoted by $t^{WEN\downarrow}_{CK\rightarrow wel\downarrow}$.
- The 3rd part represents the propagation of q_1's rising edge through Q. The input signals are q_1 and wel. The output is Q. A falling edge of wel and a rising edge of q_1, induce a rising edge on Q. The goal is to compute the lower and upper bounds of the occurence of the rising edge of Q, starting from the rising edge of CK. This will be denoted by $t^{q_1\uparrow,wel\downarrow}_{CK\rightarrow Q\uparrow}$. Using the bounds $t^{WEN\downarrow}_{CK\rightarrow wel\downarrow}$ and $t^{D\uparrow}_{CK\rightarrow q_1\uparrow}$ found in the two first parts, this will allow us finally to determine the constraints on $t^{D\uparrow,WEN\downarrow}_{CK\rightarrow Q\uparrow}$.

5.2 Generic Constraints

We analyze separately each part, thus obtaining constraints binding intermediate input and output parameters (see Appendix 2, 3, 4). The "transgressing constraints" identified during the refinement process (see Sect. 4.2) are those

incompatible with the values of the datasheet and delay intervals of $SP1$ (see Sect. 5.3). By recombination of these separate sets of constraints, we obtain constraints relating the inputs and outputs of the whole memory, that are given below. For the case of a rising edge of D, we have:

$$
\begin{array}{l}
\quad \mathit{Assumption}(D\uparrow): \\
\quad t_{setup_D} + u_2^{\downarrow} + u_3^{\downarrow} \leq l_0^{\uparrow} + t_{LO} \quad \wedge \quad u_1^{\uparrow} < t_{LO} \\
\wedge \;\; u_0^{\uparrow} + u_1^{\uparrow} < t_{setup_D} + l_2^{\downarrow} + l_3^{\downarrow} \quad \wedge \quad u_3^{\downarrow} + t_{setup_{WEN}} < t_{LO} + l_{13}^{\downarrow} \\
\wedge \;\; u_{13}^{\downarrow} + u_{14}^{\downarrow} < t_{setup_{WEN}} + l_3^{\downarrow} \quad \wedge \quad u_{13}^{\downarrow} + u_{14}^{\downarrow} + u_{16}^{\downarrow} < t_{setup_{WEN}} + l_3^{\downarrow} + l_{15}^{\downarrow} \\
\wedge \;\; u_5^{\uparrow} + u_0^{\uparrow} + u_1^{\uparrow} \leq l_8^{\downarrow} + l_3^{\downarrow} + l_{15}^{\downarrow} + t_{setup_D}
\end{array}
$$

$$
\begin{array}{l}
\quad \mathit{Final}(D\uparrow): \\
l_3^{\downarrow} + l_{15}^{\downarrow} + l_8^{\downarrow} + l_7^{\uparrow} \quad \leq \quad t_{CK\rightarrow Q\uparrow}^{D\uparrow,WEN\downarrow} \quad \leq \quad u_3^{\downarrow} + u_{15}^{\downarrow} + u_8^{\downarrow} + u_7^{\uparrow}
\end{array}
$$

In the case of a falling edge of D, the propagation of D induces a falling edge of q_1, then of Q. Accordingly $\mathit{Assumption}(D\downarrow)$ (resp. $\mathit{Final}(D\downarrow)$) can be deduced from $\mathit{Assumption}(D\uparrow)$ (resp. $\mathit{Final}(D\uparrow)$) by changing each $l_i^{\uparrow}$ (resp. $u_i^{\uparrow}$) of $\mathit{Assumption}(D\uparrow)$ (resp. $\mathit{Final}(D\uparrow)$) into $l_i^{\downarrow}$ (resp. $u_i^{\downarrow}$).

From $\mathit{Final}(D\uparrow)$ and $\mathit{Final}(D\downarrow)$, we infer the following constraint, guaranteeing property $t_{CK\rightarrow Q}^{D,WEN\downarrow} \leq t_{max}^{write}$:

$$\boxed{u_3^{\downarrow} + u_{15}^{\downarrow} + u_8^{\downarrow} + \max\{u_7^{\uparrow}, u_7^{\downarrow}\} \leq t_{max}^{write}.} \qquad (*)$$

Constraints of $\mathit{Assumption}(D\uparrow)$ and $\mathit{Assumption}(D\downarrow)$ can be used to determine lower and upper bounds for t_{setup_D}:

$$
\begin{array}{l}
\max\{u_0^{\uparrow} + u_1^{\uparrow} + u_5^{\uparrow} - l_8^{\downarrow} - l_3^{\downarrow} - l_{15}^{\downarrow}, u_0^{\downarrow} + u_1^{\downarrow} + u_5^{\downarrow} - l_8^{\downarrow} - l_3^{\downarrow} - l_{15}^{\downarrow}, \\
\quad u_0^{\uparrow} + u_1^{\uparrow} - l_2^{\downarrow} - l_3^{\downarrow}, u_0^{\downarrow} + u_1^{\downarrow} - l_2^{\downarrow} - l_3^{\downarrow}\} \quad \leq \quad t_{setup_D} \\
\wedge \;\; t_{setup_D} \leq t_{LO} + l_0^{\uparrow} - u_2^{\downarrow} - u_3^{\downarrow}
\end{array}
$$

We thus infer an *optimal* value of t_{setup_D}, denoted by $t_{setup_D}^{opt}$, which corresponds to its lower bound[8] of the form $t_{setup_D}^{opt} = \max\{t_{D1}^{opt}, t_{D2}^{opt}\}$ with:

$$\boxed{t_{D1}^{opt} = \max\{u_0^{\uparrow} + u_1^{\uparrow} + u_5^{\uparrow}, u_0^{\downarrow} + u_1^{\downarrow} + u_5^{\downarrow}\} - l_8^{\downarrow} - l_3^{\downarrow} - l_{15}^{\downarrow}\}}$$

$$\boxed{t_{D2}^{opt} = \max\{u_0^{\uparrow} + u_1^{\uparrow}, u_0^{\downarrow} + u_1^{\downarrow}\} - l_2^{\downarrow} - l_3^{\downarrow}}$$

A similar expression can be obtained for the optimal value of $t_{setup_{WEN}}$.

Remark. Although the coefficients appearing in the linear expressions of constraints $\mathit{Assumption}(D\uparrow)$ and $\mathit{Final}(D\downarrow)$ are all equal to ± 1, this is not the

[8] Actually, we checked that $t_{setup_D}^{opt}$ also satisfies constraints, coming from other parts of the circuit, which are not limitative in the case of instances $SP1$ and $SP2$.

case of many coefficients appearing in the intermediate constraints generated by $Post^{2t_{cycle}}(Assumption(D\uparrow))$. This is an important difference of our approach with the framework of [9, 8], where all the constraints are upper approximated as "octahedra" (linear constraints with coefficients ± 1).

5.3 Application to Instance *SP*1

The above sets of constraints now allow us to give a formal justification of the correctness of the instance $SP1$. The values of the datasheet are (in tens of picoseconds):

$t_{HI} = 36, t_{LO} = 74, t_{setup_D} = 108, t_{setup_{WEN}} = 48, t_{max}^{write} = 56.$

The internal delays are (in tens of picoseconds):

	$[l_i^{\uparrow}, u_i^{\uparrow}]$	$[l_i^{\downarrow}, u_i^{\downarrow}]$
(l_0, u_0)	$(95, 95)$	$(66, 66)$
(l_1, u_1)	$(14, 14)$	$(18, 18)$
(l_2, u_2)	$(23, 30)$	$(23, 30)$
(l_3, u_3)	$(5, 5)$	$(2, 2)$
(l_5, u_5)	$(22, 22)$	$(45, 45)$
(l_7, u_7)	$(21, 21)$	$(20, 20)$
(l_8, u_8)	$(0, 0)$	$(22, 22)$
(l_{13}, u_{13})	$(11, 11)$	$(8, 8)$
(l_{14}, u_{14})	$(21, 22)$	$(21, 22)$
(l_{15}, u_{15})	$(14, 14)$	$(11, 11)$
(l_{16}, u_{16})	$(24, 24)$	$(0, 0)$

We check that all the constraints of $Assumption(D\uparrow)$, and $Assumption(D\downarrow)$, as well as $(*)$ are satisfied. This guarantees that $SP1$ satisfies $t_{CK\to Q}^{D,WEN^{\uparrow}} \leq t_{max}^{write}$. Furthermore, we find the value 96 for $t_{setup_D}^{opt}$, which matches very well with the optimal value 95 found by simulation by the designer.

5.4 Application to Instance *SP*2

As mentioned in Sect. 5.2, the values of the datasheet and internal delays of $SP1$ have been used in the refinement process to identify transgressing inequalities, and guide the derivation of constraints $Assumption(D\uparrow)$, $Assumption(D\downarrow)$ and $(*)$. The same constraints can now be reused directly to verify other implementations. In other words, any implementation of SPSMALL whose values satisfy these constraints, is guaranteed to be correct (with respect to the write property). This is what happens with $SP2$. The values of the datasheet of $SP2$ are indeed (in tens of picoseconds):

$t_{HI} = 72, t_{LO} = 170, t_{setup_D} = 241, t_{setup_{WEN}} = 109, t_{max}^{write} = 142.$

The internal delays are (in tens of picoseconds):

	$[l_i^{\uparrow}, u_i^{\uparrow}]$	$[l_i^{\downarrow}, u_i^{\downarrow}]$
(l_0, u_0)	$(197, 197)$	$(140, 140)$
(l_1, u_1)	$(60, 60)$	$(58, 58)$
(l_2, u_2)	$(66, 66)$	$(43, 43)$
(l_3, u_3)	$(8, 8)$	$(4, 4)$
(l_5, u_5)	$(61, 61)$	$(63, 63)$
(l_7, u_7)	$(47, 47)$	$(52, 52)$
(l_8, u_8)	$(0, 0)$	$(42, 42)$
(l_{13}, u_{13})	$(23, 23)$	$(23, 23)$
(l_{14}, u_{14})	$(35, 35)$	$(36, 36)$
(l_{15}, u_{15})	$(56, 56)$	$(43, 43)$
(l_{16}, u_{16})	$(24, 24)$	$(0, 0)$

It is easy to check that these values satisfy *Assumption*($D\uparrow$), *Assumption*($D\downarrow$) and $(*)$. Furthermore, the value of $t^{opt}_{setup_D}$ for $SP2$ can be found, as explained in Sect. 5.2. This gives $t^{opt}_{setup_D} = 229$, which matches exactly with the optimal value found by electrical simulation by the designer.

5.5 Interpretation of *Assumption* and *Final* constraints

Let us explain how certain constraints of *Assumption* and *Final* can be interpreted. As mentioned above, the constraints of *Final* is of the form $f(l, u) \leq t^{D,WEN\downarrow}_{CK\rightarrow Q} \leq g(l, u)$, where $g(l, u)$ is a sum of internal delays (viz. $u_3^{\downarrow} + u_{15}^{\downarrow} + u_8^{\downarrow} + \max\{u_7^{\uparrow}, u_7^{\downarrow}\}$), and similarly for $f(l, u)$. This expression corresponds to the delay associated to the path which starts at input CK, goes through inverter not_3, then wires $wire_{15}$, $wire_8$, $wire_7$, and ends at output port Q. Such a path is *critical*, as it corresponds to the longest traversal from an input to the output port Q, thus conditioning the end-to-end delay to Q. This feature is guaranteed by the set of constraints *Assumption*, which gives conditions, among others, enquiring the other paths to be shorter. More precisely, the constraints in the set *Assumption* state:

- the order along which signals arrive at junction points (logical gates or blocks). For instance, inequality $u_5^{\uparrow} + u_0^{\uparrow} + u_1^{\uparrow} \leq l_8^{\downarrow} + l_3^{\downarrow} + l_{15}^{\downarrow} + t_{setup_D}$ says that, at junction point *output buffer*, the input o_5 (issued from a rising edge of D, occurring t_{setup_D} before the rising edge of CK, and following path $wire_0$-$latch_D$-$wire_5$) arrives before input o_8 (issued from a rising edge of CK, and following path not_3-$wire_{15}$-$wire_8$); in other words, this inequality says that the data to be written in the output buffer arrives before the writing command.
- the stability conditions sufficient to ensure that an input signal correctly propagates throughout a component. For instance, inequality $u_0^{\uparrow} + u_1^{\uparrow} \leq t_{setup_D} + l_2^{\downarrow} + l_3^{\downarrow}$ says that input d_1 (issued from the rising edge of D, occurring t_{setup_D} before the rising edge of CK) arrives at least u_1 before input e_{l_D} of $latch_D$ (issued from the rising edge of CK, and following path not_3-$wire_2$); in other words, the inequality says that the data to be latched arrives early enough before the latch closes.

6 Verification of the Read Property

In this Section, we focus on the *read* operation (instead of *write*). The relevant portion of the circuit (in case of a falling edge of A) is depicted on Fig. 8. Recall that we assume that the port of A is reduced to a single bit. Furthermore, the $m \times n$ storage array is abstracted as a unique memory point mp. As mentioned before, the operations involving the memory points may take different times, according to the physical location of the memory point. We will assume that mp corresponds to the memory point taking the *longest* time (i.e., the one corresponding to the "slowest" $wire_{10}$)[9]. Moreover, input D is not relevant for this property.

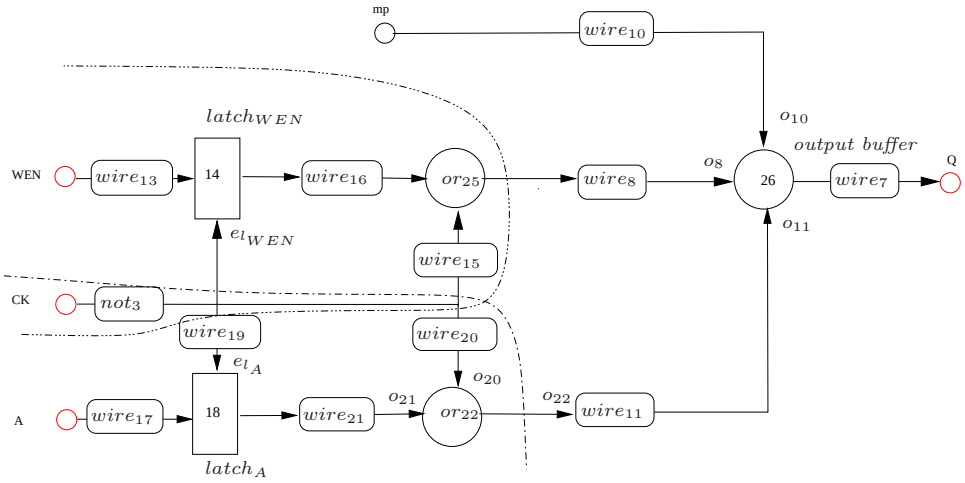

Fig. 8. Schematics of the relevant portion of SPSMALL for read.

The "response time" property for the read operation now expresses as follows:

$$t_{CK\to Q}^{A\downarrow,WEN\uparrow} \leq t_{max}^{read} \text{ and } t_{CK\to Q}^{A\uparrow,WEN\uparrow} \leq t_{max}^{read}.$$

We now focus on the case of a falling edge of A. (A similar approach applies for the rising edge case.) The timing parameters involved are depicted on Fig. 9. As for the write property, the schematics decomposes itself into three subparts (delimited by the dashed line on Fig. 8). Likewise, the analysis is performed on each subpart, and the associated constraints recombined together. The resulting constraints (besides $\{l_i^{\downarrow} \leq u_i^{\downarrow}\}$ and $\{l_i^{\uparrow} \leq u_i^{\uparrow}\}$) are:

Assumption($A\downarrow$):

[9] Such a memory point generally corresponds to an "extreme" point of the topology of the memory array, and can be identified by electrical simulation.

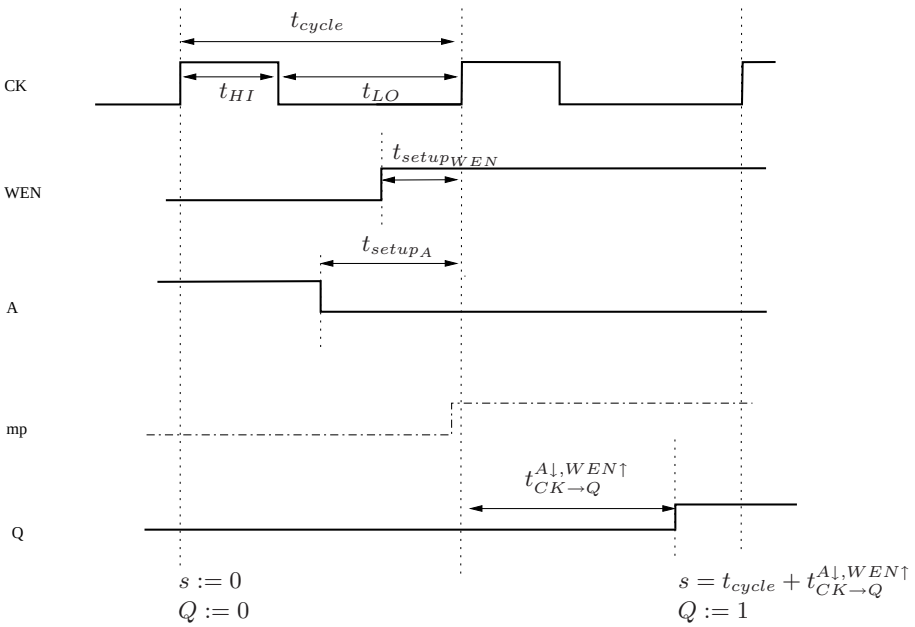

Fig. 9. Timing diagram for the *read* operation (considering mp = 1 at the beginning of the cycle of the read operation).

$$\max\{u^{\uparrow}_{10}, u^{\downarrow}_{10}\} < l^{\downarrow}_{3} + l^{\downarrow}_{20} + l^{\downarrow}_{11} \quad \wedge \quad t_{LO} + l^{\downarrow}_{17} > u^{\downarrow}_{3} + u^{\downarrow}_{19} + t_{setup_A}$$
$$\wedge\ u^{\downarrow}_{17} + u^{\downarrow}_{18} < t_{setup_A} + l^{\downarrow}_{3} + l^{\downarrow}_{19} \ \wedge\ u^{\downarrow}_{18} < t_{LO} \ \wedge\ u^{\downarrow}_{17} + u^{\downarrow}_{18} + u^{\downarrow}_{21} < t_{setup_A} + l^{\downarrow}_{3} + l^{\downarrow}_{20}$$
$$\wedge\ t_{LO} + l^{\uparrow}_{13} > u^{\downarrow}_{3} + t_{setup_{WEN}} \quad \wedge \quad u^{\uparrow}_{13} + u^{\uparrow}_{14} < t_{setup_{WEN}} + l^{\downarrow}_{3}$$
$$\wedge\ u^{\uparrow}_{13} + u^{\uparrow}_{14} + u^{\uparrow}_{16} < t_{setup_{WEN}} + l^{\downarrow}_{3} + l^{\downarrow}_{15}$$

Final$(A\downarrow)$:

$$l^{\downarrow}_{3} + l^{\downarrow}_{20} + l^{\downarrow}_{11} + \max\{l^{\downarrow}_{7}, l^{\uparrow}_{7}\} \ \leq \ t^{A\downarrow,WEN\uparrow}_{CK\to Q} \ \leq \ u^{\downarrow}_{3} + u^{\downarrow}_{20} + u^{\downarrow}_{11} + \max\{u^{\downarrow}_{7}, u^{\uparrow}_{7}\}$$

Similarly, one can infer sets *Assumption*$(A\uparrow)$ and *Final*$(A\uparrow)$. From *Final*$(A\downarrow)$ and *Final*$(A\uparrow)$, we infer the following constraint, guaranteeing $t^{A,WEN\uparrow}_{CK\to Q} \leq t^{read}_{max}$:

$$\boxed{u^{\downarrow}_{3} + u^{\downarrow}_{20} + u^{\downarrow}_{11} + \max\{u^{\uparrow}_{7}, u^{\downarrow}_{7}\} \leq t^{read}_{max}.} \qquad (**)$$

Constraints of *Assumption*$(A\downarrow)$ and *Assumption*$(A\uparrow)$ can be used to infer an *optimal* value of t_{setup_A}, denoted by $t^{opt}_{setup_A}$[10], of the form $t^{opt}_{setup_A} = \max\{t^{opt}_{A1}, t^{opt}_{A2}\}$ with:

$$\boxed{t^{opt}_{A1} = \max\{u^{\downarrow}_{17} + u^{\downarrow}_{18} + u^{\downarrow}_{21}, u^{\uparrow}_{17} + u^{\uparrow}_{18} + u^{\uparrow}_{21}\} - l^{\downarrow}_{3} - l^{\downarrow}_{20}}$$

[10] Actually, we checked that $t^{opt}_{setup_A}$ also satisfies constraints, coming from other parts of the circuit, which are not limitative in the case of instances $SP1$ and $SP2$.

$$\boxed{t_{A2}^{opt} = \max\{u_{17}^{\downarrow} + u_{18}^{\downarrow}, u_{17}^{\uparrow} + u_{18}^{\uparrow}\} - l_{3}^{\downarrow} - l_{19}^{\downarrow}\}}$$

As in Sect. 5.5, the constraints of *Final* correspond to the delays associated with the critical path: it is issued from CK, goes through not_3, $wire_{20}$, $wire_{11}$ and $wire_7$. Likewise, many constraints of *Assumption* can be viewed as sufficient conditions either for the other paths to be shorter than the critical one, or for the input signals to propagate through all the components to Q.

Verification of $SP1$. The relevant values of the datasheet $SP1$ (in tens of picoseconds) :

$t_{HI} = 36, t_{LO} = 74, t_{setup_A} = 58, t_{max}^{read} = 77$
The internal delays are (in tens of picoseconds):

	$[l_i^{\uparrow}, u_i^{\uparrow}]$	$[l_i^{\downarrow}, u_i^{\downarrow}]$
(l_3, u_3)	$(5, 5)$	$(2, 2)$
(l_7, u_7)	$(21, 21)$	$(20, 20)$
(l_{10}, u_{10})	$(6, 6)$	$(6, 6)$
(l_{11}, u_{11})	$(23, 23)$	$(23, 23)$
(l_{13}, u_{13})	$(11, 11)$	$(8, 8)$
(l_{14}, u_{14})	$(21, 22)$	$(21, 22)$
(l_{16}, u_{16})	$(24, 24)$	$(0, 0)$
(l_{17}, u_{17})	$(16, 16)$	$(15, 15)$
(l_{18}, u_{18})	$(31, 31)$	$(31, 31)$
(l_{19}, u_{19})	$(15, 15)$	$(12, 12)$
(l_{20}, u_{20})	$(40, 40)$	$(29, 29)$
(l_{21}, u_{21})	$(0, 0)$	$(0, 0)$

We check that all the constraints of *Assumption*($A\downarrow$), *Assumption*($A\uparrow$) and $(**)$ are satisfied. This guarantees that $SP1$ satisfies $t_{CK\rightarrow Q}^{A,WEN\uparrow} \leq t_{max}^{read}$. Furthermore, we find the value 30 for $t_{setup_A}^{opt}$, which matches exactly with the optimal value found by simulation by the designer.

Verification of $SP2$. Similarly to what has been explained in Sect. 5.4, the above constraints *Assumption*($A\downarrow$), *Assumption*($A\uparrow$) and $(**)$, whose derivation was guided by the values of $SP1$, can be reused directly to verify the the read property of others implementations. In the case of $SP2$, the values of the datasheet of are (in tens of picoseconds):

$t_{HI} = 72, t_{LO} = 170, t_{setup_A} = 110, t_{max}^{read} = 169$
The internal delays are (in tens of picoseconds):

	$[l_i^{\uparrow}, u_i^{\uparrow}]$	$[l_i^{\downarrow}, u_i^{\downarrow}]$
(l_3, u_3)	$(8, 8)$	$(4, 4)$
(l_7, u_7)	$(47, 47)$	$(52, 52)$
(l_{10}, u_{10})	$(14, 14)$	$(10, 10)$
(l_{11}, u_{11})	$(51, 51)$	$(55, 55)$
(l_{13}, u_{13})	$(23, 23)$	$(23, 23)$
(l_{14}, u_{14})	$(35, 35)$	$(36, 36)$
(l_{16}, u_{16})	$(24, 24)$	$(0, 0)$
(l_{17}, u_{17})	$(14, 14)$	$(9, 9)$
(l_{18}, u_{18})	$(79, 79)$	$(89, 89)$
(l_{19}, u_{19})	$(36, 36)$	$(22, 22)$
(l_{20}, u_{20})	$(74, 74)$	$(58, 58)$
(l_{21}, u_{21})	$(0, 0)$	$(0, 0)$

It is easy to check that $Assumption(A\downarrow)$, $Assumption(A\uparrow)$ and $(**)$ are satisfied by these values. Besides, we find the value 75 for $t^{opt}_{setup_A}$, which matches well with the optimal value (74) found by electrical simulation by the designer.

7 Final Remarks

We have shown in this paper how to apply parameterized methods to verify timed properties of the generic architecture of a memory. We have thus found certain sufficient conditions (under the form of linear inequalities between parameters) that ensure that the response times to a write command or a read command lie between certain bounds, and have checked these properties on an instance $SP1$ of the memory. These linear inequalities have been also used to derive the optimal values of setup timings of input signals (*viz.*, setup timings for D and A). Such an analysis can be immediately applied to the verification of other instances of the SPSMALL memory, as examplified here on instance $SP2$.

Other properties concerning the writing into the memory points, and concerning the "hold timings" of input signals (minimal stability duration after the rising edge of the clock) can be proved similarly, for the completion of the verification. Note that such properties are considered by the designer as less sensitive for the SPSMALL architecture.

Let us also point out that our verification process does not get rid completely of results given by simulation, since it makes use of values of *elementary* delays $[l^{\downarrow}, u^{\downarrow}]$ and $[l^{\uparrow}, u^{\uparrow}]$ for the internal components. This is in contrast with the traditional simulation process, which computes the values of the *end-to-end* propagation delays setting up the datasheet.

Our method has exploited the data available for instance $SP1$ (datasheet and internal delay intervals), especially during the stepwise refinement process, when we identify peculiar subconstraints (the "transgressing inequalities"). By negating such subconstraints, we have actually focused on a certain class of the

circuit, disregarding other possible choices of implementation. In fact, the major outcome of our verification process is a general and formal description of the architecture principles along which SPSMALL has been designed. We have shown that these principles are correctly implemented by two different instances of the memory.

Let us finally point out that our method of verification relies on *forward* reachability analysis (generation of successor states starting from the initial one). A promising alternative is to use *backward* reachability analysis (generation of predecessor states, starting from a final one). This is the subject of on-going research.

References

1. HSIM Simulator Description. In `http://www.synopsys.com/products/`.
2. TLL Transistor Abstraction Tool description. In `http://www.transeda.com/products/`.
3. R. Alur and D.L. Dill. A theory of timed automata. *Theoretical Computer Science 126*, pages 183–235, 1994.
4. M. Baclet and R. Chevallier. Timed verification of the SPSMALL memory. In *1th International Conference Memory Technology and Development*, pages 1–2, Giens France, 2005.
5. M. Bozga, H. Jianmin, O. Maler, and S. Yovine. Verification of asynchronous circuits using timed automata. In *TPTS'02, ENTCS vol 65*, 2002.
6. J.A. Brzozowski and C-J.H. Seger. *Asynchronous Circuits*. Springer, 1994.
7. R. Chevallier, E. Encrenaz-Tiphène, L. Fribourg, and W. Xu. Timing analysis of an embedded memory: SPSMALL. In *10th WSEAS International Conference on Circuits, Athens, Greece*, 2006.
8. R. Clariso and J. Cortadella. The octahedron abstract domain. In *Proc. 11th Static Analysis Symposium (SAS), LNCS 3148, Springer, pp. 312-327*, 2004.
9. R. Clariso and J. Cortadella. Verification of timed circuits with symbolic delays. In *Proc. Asia and South Pacific Design Automation Conference (ASP-DAC), pp. 628-633*, 2004.
10. P. Cousot and R. Cousot. Abstract interpretation: A unified lattice model for static analysis of programs by construction or approximation of fixpoints. In *POPL, pp. 238-252*, 1977.
11. D. Dill. Timing assumptions and verification of finite-state concurrent systems. In *Automatic Verification Methods for Finite State Systems, LNCS 407, Springer*, 1989.
12. N. Halbwachs. Delay analysis in synchronous programs. In *CAV'93, LNCS 697, Springer, pp. 333-346*, 1993.
13. T.A. Henzinger, P.-H. Ho, and H. Wong-Toi. A User Guide to HYTECH. In *TACAS'95, LNCS 1019, Springer, pp.41-71*, 1995.
14. K. Larsen, P. Pettersson, and W. Yi. UPPAAL in a Nutshell. *International Journal on Software Tools for Technology Transfer*, 1:134–152, 1997.
15. O. Maler and A. Pnueli. Timing analysis of asynchronous circuits using timed automata. In *CHARME'95, LNCS 987, Springer, pp.189-205*, 1995.
16. D.A. Patterson and J.L. Hennessy. *Computer Architecture: A Quantitative Approach*. Morgan Kaufmann, 1990.

17. R. Ben Salah, M. Bozga, and O. Maler. On timing analysis of combinational circuits. In *FORMATS'03, LNCS 2791, Springer, pp.204-219*, 2003.
18. S.Yovine. KRONOS: A verification tool for real-time systems. *International Journal on Software Tools for Technology Transfer*, 1:123–133, 1997.

Appendix 1. Memory Storage mechanism

Fig. 10 gives a closer view of the memory storage mechanism. Thick lines in the figure represent the reduced number of paths on which our analysis focus on.

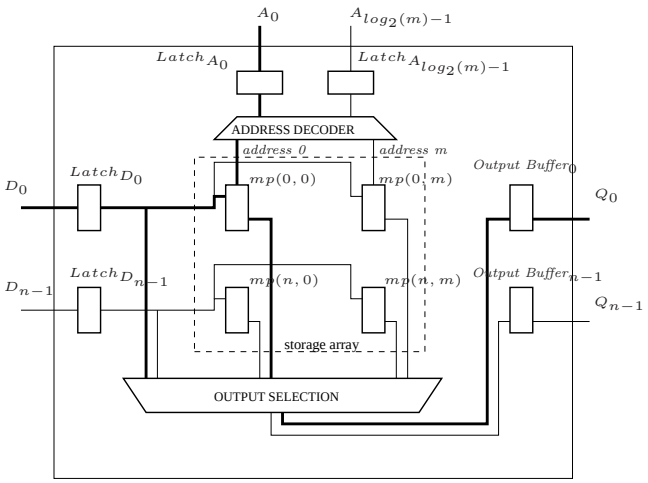

Fig. 10. Schematic view of parallel paths of D, A and Q.

Appendix 2. Computation of $t^{D}_{CK\rightarrow q_1}$

The experiment propagates an edge (either rising or falling) from D to q_1. Corresponding schematics is depicted on Fig. 11. Timing parameters are depicted on Fig. 12. Applying the constraint extraction procedure of section 4.2, we obtain, in the case of a rising edge of D ($D\uparrow$):

Assumption:
$u_0^{\uparrow} + u_1^{\uparrow} < t_{setup_D} + l_2^{\downarrow} + l_3^{\downarrow} \quad \wedge \quad u_1^{\uparrow} < t_{LO} \quad \wedge \quad t_{setup_D} + u_2^{\downarrow} + u_3^{\downarrow} \leq l_0^{\uparrow} + t_{LO}$

Final:
$t_{HI} + t_{LO} - t_{setup_D} + l_0^{\uparrow} + l_1^{\uparrow} \quad \leq \quad t^{D\uparrow}_{CK\rightarrow q_1\uparrow} \quad \leq \quad t_{HI} + t_{LO} - t_{setup_D} + u_0^{\uparrow} + u_1^{\uparrow}$

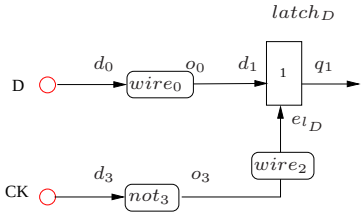

Fig. 11. Components for the computation of $t^D_{CK \to q_1}$.

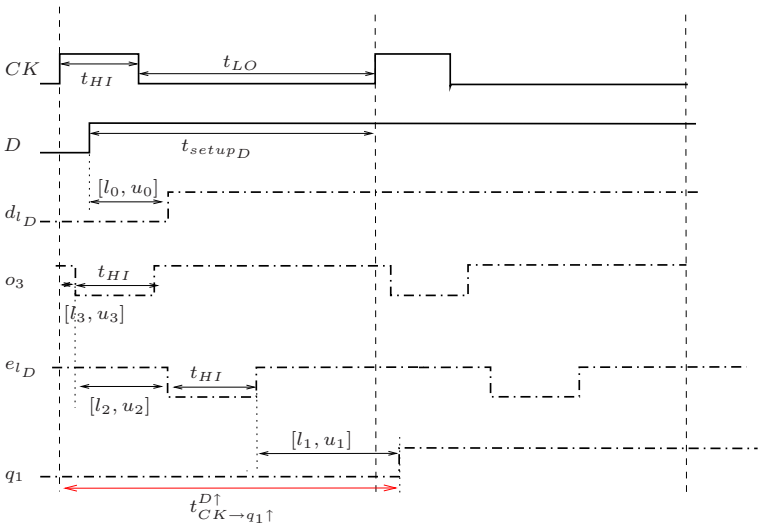

Fig. 12. Timing parameters for the computation of $t^{D\uparrow}_{CK \to q_1 \uparrow}$.

Let us sketch out on this subpart of SPSMALL how $Assumption$ and $Final$ are generated. The first step of the procedure consists in forward reachability analysis starting with $Assumption1 = True$. This yields: $Final1 = Post^{2cycle}(Assumption1)$. Among the bad states of $Final1$, we identify an inequality J of the form $u_0^{\uparrow} + u_1^{\uparrow} \geq t_{setup_D} + l_2^{\downarrow} + l_3^{\downarrow}$, which is transgressing for $SP1$ (because $95 + 14 \geq 108 + 23 + 2$ does not hold). The second step of the procedure then consists in creating $Assumption2$ by adding the negation of J to $Assumption1$, i.e.: $Assumption2 = (u_0^{\uparrow} + u_1^{\uparrow} < t_{setup_D} + l_2^{\downarrow} + l_3^{\downarrow})$. The process goes on by computing $Final2 = Post^{2cycle}(Assumption2)$, and so on, until no bad state is generated.

Appendix 3. Computation of $t_{CK \rightarrow wel\downarrow}^{WEN\downarrow}$

This experiment gives analytical expressions of lower and upper bounds of $t_{CK \rightarrow wel\downarrow}^{WEN\downarrow}$. It consists in propagating a falling edge from input port WEN up to internal signal wel. The schematics of the components is described on Fig. 13. The timing

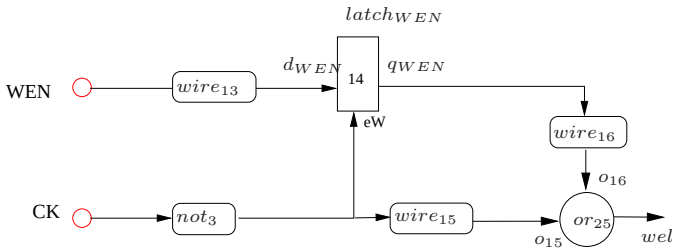

Fig. 13. Components involved in the computation of $t_{CK \rightarrow wel\downarrow}^{WEN\downarrow}$.

parameters are defined on Fig. 14. Applying the constraint extraction procedure of section 4.2, we obtain:

Assumption:
$t_{LO} + l_{13}^{\downarrow} > u_3^{\downarrow} + t_{setup_{WEN}} \quad \wedge \quad u_{13}^{\downarrow} + u_{14}^{\downarrow} < t_{setup_{WEN}} + l_3^{\downarrow}$
$\wedge \quad u_{13}^{\downarrow} + u_{14}^{\downarrow} + u_{16}^{\downarrow} < t_{setup_{WEN}} + l_3^{\downarrow} + l_{15}^{\downarrow}$

Final:
$l_3^{\downarrow} + l_{15}^{\downarrow} \quad \leq \quad t_{CK \rightarrow wel}^{WEN} \quad \leq \quad u_3^{\downarrow} + u_{15}^{\downarrow}$

Appendix 4. Computation of $t_{CK \rightarrow Q}^{q_1, wel\downarrow}$

The experiment propagates a rising (resp. falling) edge from q_1 , occuring at instant $t_{CK \rightarrow q_1\uparrow}^{D\uparrow}$ (resp. $t_{CK \rightarrow q_1\downarrow}^{D\downarrow}$), up to the output port Q. Signal wel is abstracted

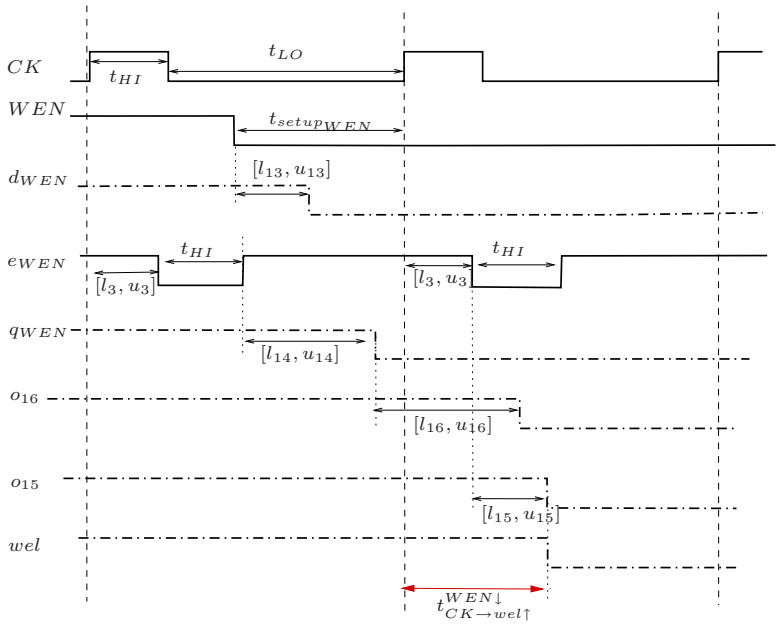

Fig. 14. Timing parameters for $t^{WEN\downarrow}_{CK\rightarrow wel\downarrow}$.

as a falling edge occuring at instant $t^{WEN\downarrow}_{CK\rightarrow wel^{\downarrow}}$. Corresponding schematics is depicted on Fig. 15. We obtain the following sets of constraints :

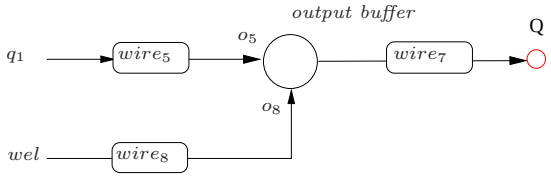

Fig. 15. Computation of $t^{q_1^{\uparrow},wel\downarrow}_{CK\rightarrow Q^{\uparrow}}$.

Assumption:
$u_5^{\uparrow} + t^{D\uparrow}_{CK\rightarrow q_1\uparrow} \leq l_8^{\downarrow} + t^{WEN\downarrow}_{CK\rightarrow wel\downarrow} + t_{HI} + t_{LO}$

Final:
$l_8^{\downarrow} + t^{WEN\downarrow}_{CK\rightarrow wel\downarrow} + l_7^{\uparrow} + t_{HI} + t_{LO} \leq t^{q_1\uparrow,wel\downarrow}_{CK\rightarrow Q\uparrow} \leq u_8^{\downarrow} + t^{WEN\downarrow}_{CK\rightarrow wel\downarrow} + u_7^{\uparrow} + t_{HI} + t_{LO}$